Chin. Sci. Bull. (2014) 59(36):5278–5282
DOI 10.1007/s11434-014-0635-5

csb.scichina.com
www.springer.com/scp

Article

Condensed Matter Physics

Compression behavior of $Sm_2Ti_2O_7$-pyrochlore up to 50 GPa: single-crystal X-ray diffraction and density functional theory calculations

Björn Winkler · Alexandra Friedrich · Wolfgang Morgenroth · Eiken Haussühl · Victor Milman · Chris R. Stanek · Kenneth J. McClellan

Received: 28 January 2014 / Accepted: 17 July 2014 / Published online: 10 October 2014

Abstract Single-crystal X-ray diffraction at pressures up to 50 GPa has been employed to study the compression behavior of $Sm_2Ti_2O_7$-pyrochlore. In contrast to earlier reports, we observed no pressure-induced amorphization or pressure-induced anion disorder up to 50 GPa. The experimental study has been complemented by density functional theory-based calculations. A combination of the theoretical and experimental data yields a bulk modulus of ≈185 GPa, significantly higher than a value which had been reported earlier. In comparison to earlier work, the current study provides more reliable data due to the use of neon as a pressure medium, which provides a more hydrostatic pressure than the aluminum, which had been employed as a pressure medium in the earlier studies. An analysis of the compressibility of $Al_2B_2O_7$ pyrochlores shows an approximately linear dependence of the bulk modulus on the unit cell volume.

Keywords Pyrochlore · High pressure · Single crystal · X-ray diffraction · Density functional theory

SPECIAL TOPIC: High Pressure Physics

B. Winkler (✉) · A. Friedrich · W. Morgenroth · E. Haussühl
Geowissenschaften, Goethe-Universität, Altenhöferallee 1, 60438 Frankfurt am Main, Germany
e-mail: b.winkler@kristall.uni-frankfurt.de

V. Milman
Dassault Systèmes BIOVIA, 334 Science Park, Cambridge CB4 0WN, UK

C. R. Stanek · K. J. McClellan
Los Alamos National Laboratory, Los Alamos, NM 87545, USA

1 Introduction

Compounds with the composition $A_2B_2O_7$ that crystallize in the pyrochlore structure have attracted significant attention, as they display a large variety of interesting physical properties. Numerous reviews have been published, in which their crystal chemistry [1], their unusual magnetic behavior at low temperatures [2], or their use as a matrix material for nuclear waste disposal [3] have been discussed.

Several studies have been published concerning the high-pressure behavior of $A_2B_2O_7$ pyrochlores, but generally, these studies have been limited to a qualitative interpretation of X-ray diffraction patterns or Raman spectra [4–10]. Specifically, the high-pressure behavior of $Sm_2Ti_2O_7$ has been studied by [6] and [7]. In these two studies, a single set of X-ray diffraction measurements was interpreted to show partial amorphization at 51 GPa, and from complementary Raman measurements, it was inferred that above ≈34 GPa anion ordering occurs. The authors came to the conclusion that at 40 GPa, $Sm_2Ti_2O_7$ crystallizes in a distorted pyrochlore structure. In the powder diffraction experiment by [6] and [7] aluminum was employed as a pressure-transmitting medium, which was claimed to provide a "quasi-hydrostatic" pressure, and no pressure medium was employed in the Raman measurements.

It is well established that the critical pressures for pressure-induced structural transitions significantly depend on shear stresses transmitted by the pressure medium [11], and hence, using noble gases as pressure-transmitting media, it is possible to explore if a pressure-induced amorphization is due to the use of an unsuitable pressure medium.

Here, we present high-pressure single-crystal data which unambiguously show that when neon is employed as a

pressure medium, $Sm_2Ti_2O_7$-pyrochlore remains cubic up to at least 50 GPa and that there is no indication for any pressure-induced disorder or amorphization during cold compression. We complement the experiments by density functional theory (DFT)-based model calculations, in order to better characterize the compression mechanism and the elastic properties of $Sm_2Ti_2O_7$-pyrochlore.

2 Experimental

2.1 Growth of single crystals

$Sm_2Ti_2O_7$ single crystals were grown by the optical floating zone method in a 4-lamp (halogen) furnace. Feed rods were produced from precursor powders of 3N and 4N purity for TiO_2 and Sm_2O_3 respectively. The synthesis approach utilized in this study has been previously employed to study pyrochlores of similar composition [12].

2.2 Synchrotron X-ray diffraction experiments

A small single crystal (20 μm × 20 μm × 10 μm) of $Sm_2Ti_2O_7$ was cut from a slice of a large single crystal. The sample crystal was loaded together with ruby chips for pressure determination [13] into a hole of 110 μm diameter in a rhenium gasket preindented to a thickness of 39 μm in a Boehler–Almax diamond anvil cell equipped with conical diamonds of 300 μm culet diameters [14]. Neon was loaded at a pressure of 0.18 GPa within a pressure vessel as a pressure-transmitting medium.

Single-crystal synchrotron X-ray diffraction was performed on the General Purpose Table at the Extreme Conditions Beamline P02.2 at PETRA III (DESY-Photon Science, Germany) [15]. The synchrotron beam of 42.86 keV ($\lambda = 0.28928$ Å) was focused to a spot of about 9 μm (H) × 3 μm (V), originating from a compound refractive lens system. Diffraction images were collected at 36.4(3) and 49.9(3) GPa with a PerkinElmer XRD1621 flat-panel detector and transformed into the *CrysAlis*^{Pro} Esperanto format according to the procedure described by [16]. An ω-scan ($-23^\circ \leq \omega \leq +21^\circ$), with a step size of 1° and an exposure time of 15 s per frame followed by cleaning images collected for 25 s per frame was used. The sample-to-detector distance of 400.933 mm was calibrated using a CeO_2 standard (NIST 674a). The converted detector images were processed with the *CrysAlis*^{Pro} software package (version 171.36.28) [17] for indexing Bragg reflections, intensity data reduction, and absorption correction. Crystal structures were refined with SHELXL97-2 [18], operated using the WinGX interface [19]. The refinement parameters and some results are presented in Table 1. The weighted *R*-factor *wR* and goodness of fit *S* are based on F^2. The final refinement was carried out with anisotropic displacement parameters for all atoms. An extinction correction was applied.

Table 1 Details of the data collections, refinement results, and structural data for $Sm_2Ti_2O_7$ at high pressures

p (GPa)	36.4(3)	49.9(3)
Formula units	8	8
Space group	$Fd\bar{3}m$	$Fd\bar{3}m$
a (Å)	9.7913(11)	9.6757(16)
V (Å^3)	938.68(19)	905.8(3)
Lin. abs. coeff. (cm^{-1})	2.50	2.58
λ (Å)	0.28928	0.28928
$\mathrm{Sin}\theta_{max}/\lambda$ (Å^{-1})	0.9939	0.9847
Observed reflections	467	442
Unique reflections	122	123
Unique reflections [$I > 2\sigma(I)$]	104	105
Parameters	11	11
$R(\mathrm{int})(F^2)$	0.0306	0.0385
$R(\sigma)$	0.0192	0.0173
$R1$ [$I > 2\sigma(I)$] (e Å^{-3})	0.0278	0.0345
$wR2$	0.0738	0.0837
GoF	1.225	1.105
$\Delta\rho_{max}$ (e/Å^3)	2.28	1.99
$\Delta\rho_{min}$ (e/Å^3)	−1.70	−2.90
x (O2)	0.4205(3)	0.4202(3)
U_{eq} (Sm) (Å^2)	0.0063(3)	0.0054(3)
U_{eq} (Ti) (Å^2)	0.0027(6)	0.0012(8)
U_{eq} (O1) (Å^2)	0.0070(9)	0.0080(10)
U_{eq} (O2) (Å^2)	0.0092(5)	0.0085(5)

3 Computational details

All calculations in the current study were performed using the CASTEP package [20]. The Wu-Cohen generalized gradient approximation [21], and the "on the fly" pseudopotentials from the CASTEP database were employed throughout. The kinetic energy cutoff which defines the size of the plane-wave basis set was 800 eV. Distances between *k*-points for Brillouin zone sampling were <0.025 Å^{-1}. The elastic stiffness coefficients were obtained from stress-strain relations.

4 Results and discussion

Typical diffraction patterns at ≈50 GPa are shown in Fig. 1.

The volume–pressure relation is shown in Fig. 2. The single-crystal diffraction study allowed the determination of the one free structural parameter. Hence, in the current study, we can investigate the compression of the individual bond lengths. The pressure dependence of the individual bond lengths is shown in Fig. 3.

The agreement between the experimentally observed and theoretically predicted bond lengths is, especially at high pressures, very satisfactory. The computed elastic stiffness coefficients are $c_{11} = 312(3)$ GPa, $c_{44} = 99(4)$ GPa, $c_{12} = 124(2)$ GPa. The bulk modulus obtained from the stress-strain calculations was 187(1) GPa, in excellent agreement with the value obtained from a fit to the compression data with a third-order Birch–Murnaghan equation of state, EOS, which yielded V_o = 1056.56(4) Å^3, $B = 185.4(2)$ GPa and $B' = 4.28(1)$.

The ambient pressure volume is well established by several independent measurements (see data in [22] and [23]) as 1071 Å^3. The DFT value (1056.6 Å^3) differs from this value by 1.4 %. Similarly, the DFT calculations give volumes too small by 2.5 % and 2.8 % with respect to the corresponding experimental values at 36.4 and 49.9 GPa, respectively. In order to compensate for this systematic error, we shifted the fitted EOS curve, and Fig. 2 shows that the resultant curve describes the new experimental data well. This implies that the bulk modulus obtained from the DFT model is reliable, and hence, we conclude that a value of $B \approx 185$ GPa is to be preferred over the older value of 165 GPa [7].

The new value is more consistent with an expectation based on the general trend of $B(V)$ in $A_2B_2O_7$-pyrochlores.

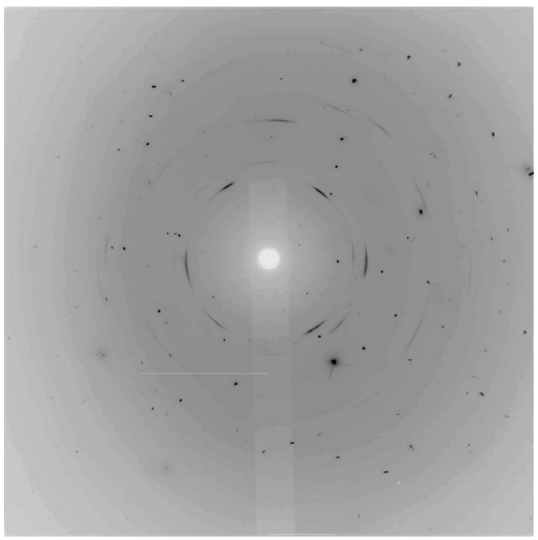

Fig. 1 Typical diffraction image collected at 50 GPa. The sharp Bragg reflections are from the $Sm_2Ti_2O_7$ crystal, while the "powder rings" are from the pressure-transmitting medium. There is no evidence of the onset of amorphization. The one very intense reflection is due to diamond

In Fig. 4 we have plotted published values of $B(A_2B_2O_7)$ as a function of unit cell volume. Chung [24] discussed that for isostructural compounds, in a first approximation, the product of the unit cell volume and bulk modulus should be constant. The scatter in the $B(V)$ relationship is to be expected, as different EOS have been used for the fits. Typically, data have been collected only at very few pressure points, and uncertainties due to the significant

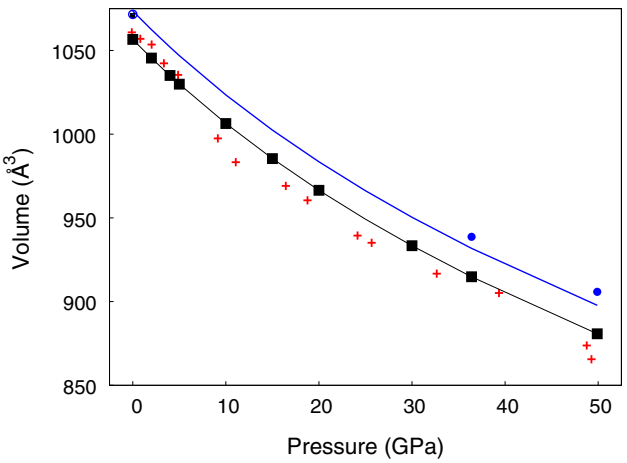

Fig. 2 (Color online) Experimental and theoretical unit cell volume–pressure relation of $Sm_2Ti_2O_7$-pyrochlore. Crosses are data from [7]. The ambient pressure cell volumes indicated by an open circle and a filled square represent independent measurements from [22] and [23]. The squares are data obtained here from DFT calculations, while the filled circles are experimental results obtained here. The curve connecting the DFT data is a fit of a third-order Birch Murnaghan equation of state, with B = 185.4(2) GPa. The other curve demonstrates that an EOS with the same B, but different V_0 describes the $V(P)$-relation of the new data points well

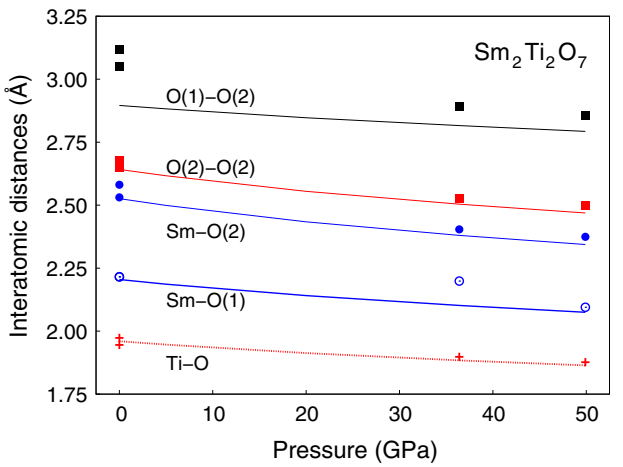

Fig. 3 (Color online) Experimental and theoretical bond distances in $Sm_2Ti_2O_7$-pyrochlore. Lines are values obtained from the DFT calculations. Data points are from experiment. The ambient pressure data points are from [23] and [22]

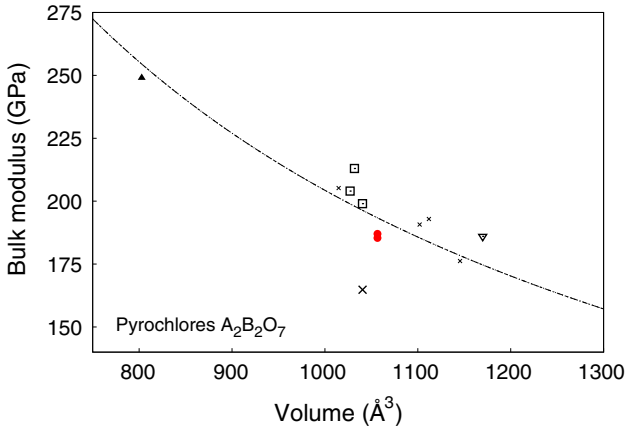

Fig. 4 (Color online) Experimental and theoretical bulk modulus-unit cell volume relations of $A_2B_2O_7$ pyrochlores. Data are from: open square: [9]; filled triangle: [10] for $MgZrSi_2O_7$; small cross: Panero et al. [25]; open triangle pointing down: [8]; large cross: Sanjay Kumar et al. [4]. The filled circles represent $B(Sm_2Ti_2O_7)$ obtained from stress-strain and compression calculations in the present study. The line is a fit to all data points, representing a relation where $B \cdot V$ = const [24]

correlation between B and B' [26] will then cause some scatter. Clearly, more data with higher accuracy are required to better understand the origin of the scatter in the $B(V)$-relation. As pyrochlores seem to be very sensitive to pressure-induced strains, it seems to be mandatory to perform new measurements with neon or helium as a pressure-transmitting medium.

Nevertheless, the available data cluster around the line describing a $B \cdot V$ = const relationship. It should be noted that we have excluded some published data. Specifically, the data by Surble et al. [5], who obtained a bulk modulus of 252(6)–255(10) GPa with $B' = 0$ for $Ce_2Zr_2O_7$, as the latter value is unphysical. Also, Surble et al. [5] found that for $Nd_2Zr_2O_7$ B = 140–145 GPa with B' = 11–14. This is puzzling, as Surble et al. [5] observed a pressure-induced structural phase transition. If the high-pressure phase would be due to a displacive phase transition, one would expect an elastic softening of the low-pressure phase close to the transition pressure. If the phase transition is reconstructive, as seems to be implied by the 19 % volume decrease and the large pressure interval over which the high- and low-pressure phase coexist, a very large B' would be very unusual.

Theoretical data, e.g., by [27] or [28], are also systematically displaced with respect to the curve shown in Fig. 4 and hence have also been excluded. It is well known that in stress-strain calculations the choice of the *xc*-functional may lead to a systematic deviation from experiment, and a further reason for systematic deviations is that the elastic behavior of compounds is generally computed in the athermal limit, while the experimental data points are collected at ambient temperature.

5 Conclusion

The current study convincingly demonstrates that there is no pressure-induced amorphization or anion disordering in $Sm_2Ti_2O_7$ at pressures up to 50 GPa on cold compression when using neon as a pressure-transmitting medium. Hence, the findings of [6] and [7] concerning the pressure-induced amorphization and anion disorder are likely to be due to the use of aluminum as a pressure-transmitting medium. The bulk modulus of $Sm_2Ti_2O_7$ is ≈185 GPa, and the pressure derivative of the bulk modulus is slightly larger than 4. As pyrochlores seem to be very sensitive to nonhydrostatic conditions, neon or helium should be employed in future experiments.

Acknowledgments This work was supported by the DFG, Germany, within SPP1236 (FR-2491/2-1), the BMBF, Germany (05KS7RF1, 05K10RFA), and DESY, Germany. Portions of this research were carried out at the light source PETRA III at DESY, a member of the Helmholtz Association (HGF). We thank H.-P. Liermann (PETRA III) for support at the beamline.

References

1. Aleshin E, Roy R (1962) Crystal chemistry of pyrochlore. J Am Ceram Soc 45:18–25
2. Gardner JS, Gingras MJP, Greedan JE (2010) Rev Mod Phys 82:53–107
3. Ewing RC, Weber WJ, Lian J (2004) Nuclear waste disposal—pyrochlore ($A_2B_2O_7$): nuclear waste form for the immobilization of plutonium and minor actinides. J Appl Phys 95:5949
4. Sanjay Kumar NR, Chandra Shekar NV, Sahu PC (2008) Pressure induced structural transformation of pyrochlore $Gd_2Zr_2O_7$. Solid State Commun 147:357–359
5. Surble S, Heathman S, Raison PE et al (2010) Pressure-induced structural transition in $Ln_2Zr_2O_7$ (Ln = Ce, Nd, Gd) pyrochlores. Phys Chem Miner 37:761–767
6. Zhang FX, Saxena SK (2005) Structural changes and pressure-induced amorphization in rare earth titanates $RE_2Ti_2O_7$ (RE: Gd, Sm) with pyrochlore structure. Chem Phys Lett 413:248–251
7. Zhang FX, Manoun B, Saxena SK et al (2005) Structure change of pyrochlore $Sm_2Ti_2O_7$ at high pressures. Appl Phys Lett 86:181906
8. Zhang FX, Lian J, Becker U et al (2007) Structural distortions and phase transformations in $Sm_2Zr_2O_7$ pyrochlore at high pressures. Chem Phys Lett 441:216–220
9. Scott PR, Midgley A, Musaev O et al (2011) High-pressure synchrotron X-ray diffraction study of the pyrochlores: $Ho_2Ti_2O_7$, $Y_2Ti_2O_7$ and $Tb_2Ti_2O_7$. High Pressure Res 31:219–227
10. Zhai S, Shan S, Yamazaki D et al (2013) Compressibility of pyrochlore-type $MgZrSi_2O_7$ determined by in situ X-ray diffraction in a large-volume high pressure apparatus. High Pressure Res 33:1–7
11. Bayarjargal L, Wiehl L, Winkler B (2013) Influence of grain size, surface energy, and deviatoric stress on the pressure-induced phase transition of ZnO and AlN. High Pressure Res 33:642–651
12. Sickafus KE, Minervini L, Grimes RW et al (2000) Radiation tolerance of complex oxides. Science 289:748–751
13. Mao HK, Xu J, Bell PM (1986) Calibration of the ruby pressure gauge to 800 kbar under quasi-hydrostatic conditions. J Geophys Res 91:4673–4676

14. Boehler R (2006) New diamond cell for single-crystal X-ray diffraction. Rev Sci Instrum 77:115103
15. Liermann H, Morgenroth W, Ehnes A et al (2010) The Extreme Conditions beamline at PETRA III, DESY: possibilities to conduct time resolved monochromatic diffraction experiments in dynamic and laser heated DAC. J Phys Conf Ser 215:012029
16. Rothkirch A, Gatta GD, Meyer M et al (2013) Single-crystal diffraction at the Extreme Conditions beamline P02.2: procedure for collecting and analyzing high-pressure single-crystal data. J Synchrotron Radiat 20:711–720
17. Agilent (2013) *CrysAlis*^{Pro} software system, version 171.36.28. Agilent Technologies UK Ltd, Oxford
18. Sheldrick GM (2008) A short history of SHELX. Acta Crystallogr A64:112–122
19. Farrugia LJ (1999) WinGX suite for small-molecule single-crystal crystallography. J Appl Crystallogr 32:837
20. Clark SJ, Segall MD, Pickard CJ et al (2005) First principles methods using CASTEP. Z Kristallogr 220:567–570
21. Wu ZG, Cohen RE (2006) More accurate generalized gradient approximation for solids. Phys Rev B 73:235116
22. Knop O, Brisse F, Castelliz L et al (1969) Thermoanalytic, X-ray, neutron, infrared, and dielectric studies of $A_2Ti_2O_7$ titanates. Can J Chem 47:971–990
23. Tabira Y, Withers RL (1999) The determination of an unknown oxygen atom position in rare-earth zirconate pyrochlores by a 111 systematic-row convergent-beam electron diffraction technique. Philos Mag A 79:1335–1346
24. Chung DH (1972) Birch's law: why is it so good? Science 177:261–263
25. Panero WR, Stixrude L, Ewing RC (2004) First-principles calculation of defect-formation energies in the Y_2(Ti, Sn, Zr)$_2O_7$ pyrochlore. Phys Rev B 70:054110
26. Angel RJ (2000) Equations of state. Rev Miner Geochem 41:35–60
27. Pruneda JM, Artacho E (2005) First-principles study of structural, elastic, and bonding properties of pyrochlores. Phys Rev B 72:085107
28. Feng J, Xiao B, Wan CL et al (2011) Electronic structure, mechanical properties and thermal conductivity of $Ln_2Zr_2O_7$ (Ln = La, Pr, Nd, Sm, Eu and Gd) pyrochlore. Acta Mater 59:1742–1760